

## Adsorption of *N*-Allylthiourea on a Mercury Electrode: Dependence on the Supporting Electrolyte Concentration

Grażyna Dalmata and Agnieszka Nosal-Wiercińska\*

*Faculty of Chemistry, Maria Curie-Skłodowska Univeristy, 20-031 Lublin, Poland*

RECEIVED APRIL 17, 2007; REVISED NOVEMBER 15, 2007; ACCEPTED NOVEMBER 20, 2007

*Keywords*  
adsorption  
*N*-allylthiourea  
A C impedance  
mercury-drop electrode  
electrostatic parameters

Adsorption of *N*-allylthiourea at the interface mercury/ $\text{NaClO}_4$  was studied as a function of electrode charge density, adsorbate, and the supporting electrolyte bulk concentration. Experimental data from measurements of the double layer differential capacity, zero charge potential, and surface tension at the zero charge potential were used in the study. Information on *N*-allylthiourea adsorption was obtained from the values of relative surface excess, free adsorption energy, interaction constants and the electrostatic parameters of the inner layer. It was found that the adsorption parameters change together with the change of the supporting electrolyte concentration, which points to competitive adsorption of *N*-allylthiourea and  $\text{ClO}_4^-$  ions.

### INTRODUCTION

Thiourea and its alkyl derivatives are strongly adsorbed on mercury from perchlorate solutions, forming a covalent bond between sulphur and mercury, which can be described in terms of partial transfer of electrons.<sup>1–4</sup>

According to Morozow *et al.*,<sup>5</sup> adsorption of  $\text{ClO}_4^-$  ions is practically eliminated in the presence of thiourea, allowing omission of coadsorption of thiourea and the supporting electrolyte ions. However, it can be concluded from the papers of Damaskin<sup>6,7</sup> that in the range of electrode positive charges, the  $\text{ClO}_4^-$  anions penetrate between the positively charged thiourea amine groups, decreasing repulsive interaction among adsorbed thiourea molecules, which leads to increased thiourea adsorption. This points to the conclusion that there are competitive effects in perchlorate solutions, which influence both the

magnitude of adsorption and the structural arrangement of adsorbate at the interface.

Thiourea and its derivatives act as corrosion inhibitors that form a protective layer on a metal surface. These inhibitors decrease the corrosion rate by various mechanisms: (i) access of oxygen to the metal surface may be blocked; (ii) rate of dissolution of the protective layer on the metal surface may be reduced; (iii) dissolution of the metal may be blocked. Polynomial model of the inhibition mechanism of thiourea derivatives was presented by Lukovits.<sup>8</sup>

Adsorption studies of substances acting as corrosion inhibitors allow for diversification of the chemical nature of the interface according to need. When a sulphur containing species has also an unsaturated aliphatic chain, one can expect that the adsorption will depend on both the sulphur end of the molecule and the properties

\* Author to whom correspondence should be addressed. (E-mail: anosal@hermes.umcs.lublin.pl)

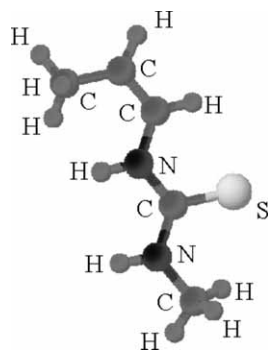


Figure 1. The molecular structure of *N*-allylthiourea.

of the aliphatic chain, *i.e.*, the existence of  $\pi$  electrons and its hydrophobicity. Allylthiourea is one of such compounds.

In the present work, we examine the adsorption of allylthiourea (ATU) on a mercury electrode from aqueous solutions of  $\text{NaClO}_4$  as a function of the concentration of the supporting electrolyte. Adsorption of ATU is considered to be a competitive process between the ATU molecule and  $\text{ClO}_4^-$  ions.

## EXPERIMENTAL

Analytical-grade reagents  $\text{NaClO}_4$  (Fluka) and *N*-allylthiourea were used without further purification. Solutions were prepared from fresh double-distilled water. ATU concentrations ranged from  $1 \times 10^{-4}$  to  $1 \times 10^{-2}$  mol  $\text{dm}^{-3}$ . Solutions were deaerated using high-purity nitrogen. During measurements, nitrogen was passed over the solution. The measurements were carried out at  $298 \pm 1$  K.

ATU adsorption was studied in 0.1, 1 and 5 mol  $\text{dm}^{-3}$   $\text{NaClO}_4$ ; the activity of water in these solutions was 0.995, 0.966 and 0.776, respectively.<sup>9,10</sup> The pH of the solutions was ca 5.2. Insertion of  $10^{-4}$ – $10^{-2}$  mol  $\text{dm}^{-3}$  ATU into the supporting electrolyte did not result in any pH changes. The experiments were performed in a three-electrode cell with a dropping mercury electrode made by MTM Poland as the working electrode,  $\text{Ag}/\text{AgCl}/\text{saturated NaCl}$  as the reference electrode and a platinum spiral as the counter electrode. The reference electrode was connected to the electrolytic cell via an intermediate vessel filled with the solution to be investigated.

The double layer capacity was measured at  $t = 6$  s after the drop birth using the impedance method with the Autolab frequency response analyzer (Eco Chemie). Reproducibility of average capacity measurements was  $\pm 0.5$  %. For the whole polarization range, capacity dispersion was tested at different frequencies between 200 and 1000 Hz. To obtain proper equilibrium values of differential capacity, linear dependence of capacity on the square element from frequency was extrapolated to zero frequency. This procedure assumes that the impedance of the double-layer is equivalent to a series capacity-resistance combination and that the rate of adsorption is diffusion-controlled.<sup>11</sup> The potential of zero

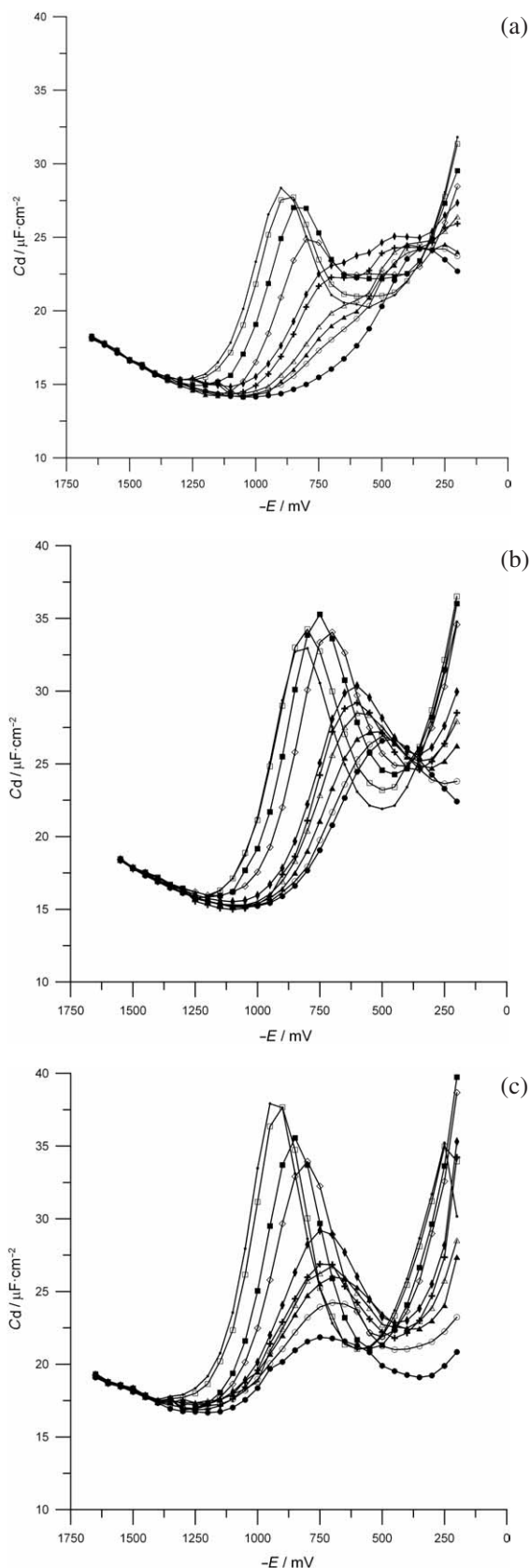


Figure 2. Differential capacity-potential curves of the mercury electrode in 0.1 mol  $\text{dm}^{-3}$  (a), 1 mol  $\text{dm}^{-3}$  (b), 5 mol  $\text{dm}^{-3}$  (c)  $\text{NaClO}_4$  with various concentrations of ATU (in  $10^{-3}$  mol  $\text{dm}^{-3}$ ) (●) 0; (○) 0.1; (▲) 0.3; (△) 0.5; (+) 0.8; (◆) 1.0; (◇) 3.0; (■) 5.0; (□) 8.0; (◊) 10.

charge ( $E_z$ ) was measured for each solution by the method of streaming mercury electrode.<sup>12,13</sup> The interfacial tension between mercury and electrolyte solutions at  $E_z$  was measured with a conventional maximum bubble-pressure capillary electrometer described earlier.<sup>14</sup> Adsorption parameters were derived by back integration of capacity-potential dependencies. No corrections were made for the effects of the medium on the activity of the supporting electrolyte<sup>15,16</sup> and the activity coefficient of the adsorbate.<sup>17</sup>

## RESULTS AND DISCUSSION

The differential capacity curves obtained in 0.1, 1 and 5 mol dm<sup>-3</sup> NaClO<sub>4</sub> for different ATU concentrations are shown in Figure 2. In solutions without ATU, the hump in the curves decreases along with increasing NaClO<sub>4</sub> concentration and is shifted to negative potentials. Together with an increase of ATU concentration, the hump is shifted to negative potentials and simultaneously the height of the hump increases. There are two reasons for the appearance of the hump in the capacity curve: reorientation of water and changes in the electrostatic interactions between adsorbed molecules.<sup>18,19</sup> A considerably smaller shift of the hump with an increase of ATU concentration in the solutions with lower water activity (Figure 2c), as well as the appearance of a small hump at low ATU concentrations in the solutions with higher water activity (Figure 2a) indicate a considerable influence of solvent on the surface properties of the interface.

Calculations of the double layer parameters for adsorption are based on the data from differential capacity-potential curves extrapolated to zero frequency. The capacity-potential plots were numerically integrated from the point of  $E_z$ . The integration constants are presented in Figure 3 and in Table I. According to Schuhmann *et al.*,<sup>20</sup> the streaming electrode does not

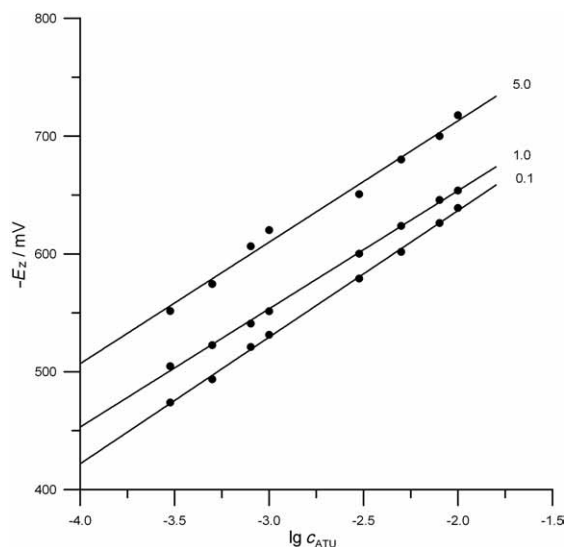


Figure 3. Dependence of the potential of zero charge vs.  $\lg c_{\text{ATU}}$  for NaClO<sub>4</sub>–ATU systems. Concentration of NaClO<sub>4</sub> (in mol dm<sup>-3</sup>) is indicated by each line.

give correct values of  $E_z$  in the ATU–0.05 mol dm<sup>-3</sup> K<sub>2</sub>SO<sub>4</sub> system. Therefore, the potentials of zero charge were also calculated from the differential capacity-potential curves integrated from the point of  $E = -1500$  mV, where it can be assumed that the ATU is totally desorbed and then the differential capacity equals the one of the supporting electrolyte solution. The differences in  $E_z$  values obtained by these two procedures did not exceed  $\pm 3$  mV. It was therefore recognized that the  $E_z$  values can be determined in perchlorate solutions by the method of streaming mercury electrode. The values of  $E_z$  measured for the solutions of NaClO<sub>4</sub> without ATU are shifted to negative potentials with an increasing NaClO<sub>4</sub> concentration, which confirms adsorption of ClO<sub>4</sub><sup>-</sup> ions. The course of  $C = f(E)$  curves in the solutions of NaClO<sub>4</sub> without ATU and the determined values of  $E_z$  are in agreement with literature data.<sup>18,19,21</sup> Introduction of ATU into the solution causes a shift of  $E_z$  values towards negative values. The linear dependence  $E_z = f(\lg c_{\text{ATU}})$  (Figure 3) points to the specific adsorption of ATU molecules on mercury.<sup>11</sup> The slope of lines  $E_z = f(\lg c_{\text{ATU}})$  is equal to 102 mV/unit  $\lg$  and is not dependent on the supporting electrolyte concentration, which indicates that ClO<sub>4</sub><sup>-</sup> ions are not specifically adsorbed.

The data obtained from the integration of differential capacity curves were subsequently used to calculate Parsons' auxiliary function  $\xi = \gamma + \sigma_M E$ ,<sup>22</sup> where  $\sigma_M$  is the electrode charge and  $E$  is the electrode potential. As the adsorption of ClO<sub>4</sub><sup>-</sup> ions was demonstrated earlier, the adsorption of ATU was described using the relative surface excess  $\Gamma'$ , which according to the Gibbs adsorption isotherm is represented by the following formula:

$$\Gamma'_{\text{ATU}} = \left( \frac{1}{RT} \right) \left( \frac{d\Phi}{d \ln c} \right)_{\sigma} \quad (1)$$

TABLE I. Surface tension  $\gamma_z$  / mN m<sup>-1</sup> for  $E_z$  of NaClO<sub>4</sub> + ATU systems

$10^3 c_{\text{ATU}} / \text{mol dm}^{-3}$	$\gamma_z / \text{mN m}^{-1}$		
	0.1 mol dm <sup>-3</sup> NaClO <sub>4</sub>	1 mol dm <sup>-3</sup> NaClO <sub>4</sub>	5 mol dm <sup>-3</sup> NaClO <sub>4</sub>
0	423.1	422.6	421.2
0.1	423.1	422.4	420.5
0.3	422.2	421.2	418.6
0.5	421.2	420.5	417.3
0.8	420.5	419.9	416.9
1.0	419.6	418.9	416.0
3.0	416.7	415.7	413.4
5.0	414.1	413.4	412.2
8.0	411.8	411.5	410.2
10.0	408.6	408.9	408.9

where  $c$  is the bulk concentration of ATU and  $\Phi$  is the surface pressure  $\Phi = \Delta\xi = \xi_0 - \xi$ , ( $\xi_0$  is the value of Parsons' auxiliary function for the supporting electrolyte and  $\xi$  is the value of Parsons' auxiliary function for the solution containing ATU). In deriving Eq. (1), it was assumed that the mean activity coefficients of  $\text{NaClO}_4$  and ATU are not changed with the change in ATU concentrations. Positive  $\Phi$  values were obtained for the studied systems most frequently in the range  $-6 \leq \sigma_M \leq +5 \mu\text{C cm}^{-2}$ .

Dependence of the relative surface excess of ATU as a function of the electrode charge and ATU concentration in the bulk obtained for  $0.1 \text{ mol dm}^{-3} \text{ NaClO}_4$  is presented in Figure 4. The  $\Gamma'$  values increase with increasing ATU concentration and electrode charge. This behaviour is common for compounds with a divalent sulphur atom, such as thiourea<sup>23</sup> and its derivatives.<sup>20,24,25</sup> The course of the curves  $\Gamma' = f(\sigma_M)$  is linear for all examined concentrations of the supporting electrolyte. Figure 5 shows the dependence of  $\Gamma'$  on the concentration of ATU and  $\text{NaClO}_4$  in bulk for the selected values of  $\sigma_M = +5, 0$  and  $-5 \mu\text{C cm}^{-2}$ . Independently of the electrode charge, the variation of  $\Gamma'$  with the ATU concentration is higher for the lower value of the concentration of ATU or supporting electrolyte presented in Figure 5. It should be noted that the  $\Gamma'$  values depend on the supporting electrolyte concentration. For ATU concentrations  $< 5 \times 10^{-4} \text{ mol dm}^{-3}$ , the values of  $\Gamma'$  increase together with an increase of  $\text{NaClO}_4$  concentration. In the presence of higher ATU concentrations, a distinct decrease of ATU surface concentration could be observed along with an increase in the supporting electrolyte concentration. An increase of the  $\text{NaClO}_4$  concentration does not only reduce the  $\Gamma'$  values, but it also changes the shape of these isotherms (this means that an increase occurs in the lateral repulsive interaction between ATU molecules when the  $\text{NaClO}_4$  concentration is higher). It is possible that the reason for such behaviour is the competitive adsorption of  $\text{ClO}_4^-$  anions on mercury. Such an effect, but to a lesser extent, was observed in the  $N,N'$ -dimethylthiourea- $\text{NaClO}_4$  system.<sup>4</sup>

### Adsorption Isotherms

Adsorption of ATU was further analyzed on the basis of the constants obtained from the Frumkin isotherm:

$$\beta x = [\Theta / (1 - \Theta)] \exp(-2A\Theta) \quad (2)$$

where  $x$  is the molar fraction of ATU in the solution,  $\beta$  is the adsorption coefficient [ $\beta = \exp(-\Delta G^\circ/RT)$ ],  $\Delta G^\circ$  is the standard Gibbs energy of adsorption,  $A$  is the interaction parameter and  $\Theta$  is the coverage,  $\Theta = \Gamma' / \Gamma_s$ .

The surface excess at saturation ( $\Gamma_s$ ) was estimated by extrapolating the  $1/\Gamma'$  vs.  $1/c_{\text{ATU}}$  at different charges to  $1/c_{\text{ATU}} = 0$ . Thus obtained surface excess at saturation

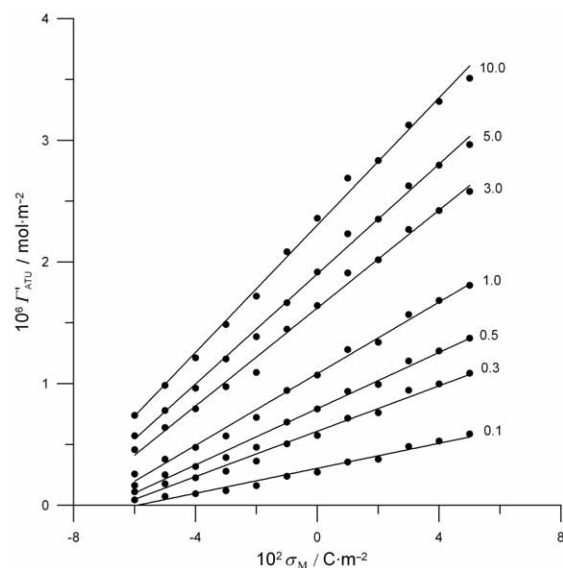


Figure 4. Relative surface excess of ATU as a function of the electrode charge and ATU concentration in the bulk for  $0.1 \text{ mol dm}^{-3} \text{ NaClO}_4$ , ATU concentrations (in  $10^{-3} \text{ mol dm}^{-3}$ ) are indicated by each line.

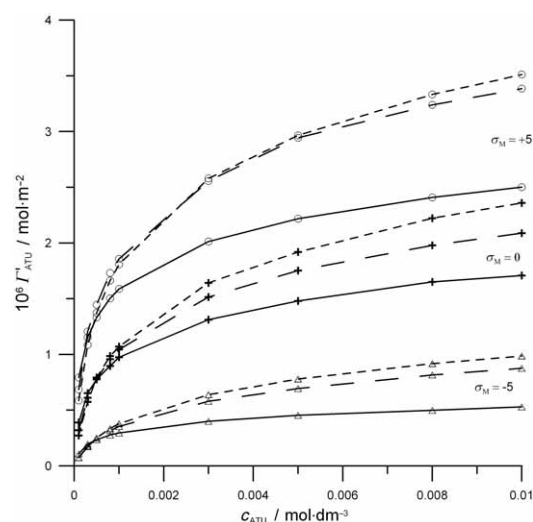


Figure 5. Relative surface excess of ATU as a function of the electrode charge and ATU concentration in the bulk for  $5 \text{ mol dm}^{-3} \text{ NaClO}_4$  (solid line),  $1 \text{ mol dm}^{-3} \text{ NaClO}_4$  (dashed line) and  $0.1 \text{ mol dm}^{-3} \text{ NaClO}_4$  (dotted line) at electrode charges:  $\sigma_M = +5 \mu\text{C m}^{-2}$  (O),  $\sigma_M = 0$  (+) and  $\sigma_M = -5 \mu\text{C m}^{-2}$  ( $\Delta$ ).

in  $0.1, 1$  and  $5 \text{ mol dm}^{-3} \text{ NaClO}_4$  is equal to  $2.96 \times 10^{-6}$ ,  $2.94 \times 10^{-6}$  and  $3.09 \times 10^{-6} \text{ mol m}^{-2}$ , respectively, which corresponds to the values of the surface occupied by one ATU molecule  $S \equiv 1 / \Gamma_s$   $0.561, 0.564$  and  $0.536 \text{ nm}^2$ . The decrease of  $S$  values with increasing  $\text{NaClO}_4$  concentration can indicate the influence of water present on the electrode surface on the results of calculations. Schuhmann *et al.*<sup>20</sup> calculated the theoretical ATU surface for several possible ATU positions assuming that ATU molecules are always arranged from sulphur towards the mercury surface. A minimal and a maximal

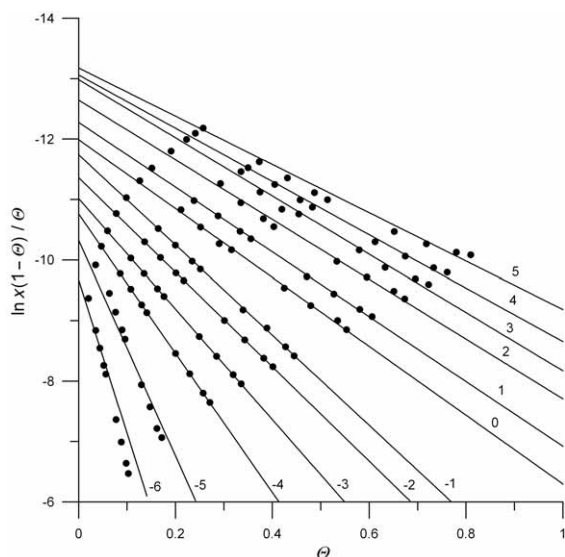


Figure 6. Linear test of the Frumkin isotherm for the system 5 mol dm<sup>-3</sup> NaClO<sub>4</sub> + ATU. Electrode charges ( $\sigma_M$  in 10<sup>-2</sup> C m<sup>-2</sup>) are indicated by each line.

surface occupied by one ATU molecule are equal, according to,<sup>20</sup> 0.27 and 0.70 nm<sup>2</sup>, respectively. According to Schuhmann,<sup>20</sup> ATU is adsorbed at more negative potentials essentially in a flat position with a resulting partial transfer of electrons located at both the sulphur atom and the double bond. When the potential becomes more positive, adsorption takes place only through the sulphur atom and thus leads to the occupation of a smaller superficial area by the molecules. The values of surfaces occupied by one ATU molecule were determined experimentally:  $S = 0.53\text{--}0.56$  nm<sup>2</sup>, which could indicate a diversion in the vertical direction of the flat position of the ATU molecule on mercury.

Figure 6 represents the linear test of the Frumkin isotherm for the system 5 mol dm<sup>-3</sup> NaClO<sub>4</sub> + ATU. The values of parameter  $A$  were calculated from the slopes of the lines of the linear test of the Frumkin isotherm. The corresponding values of  $\Delta G^\circ$  were determined by extrapolation of the line  $\ln [(1 - \theta)x / \theta]$  vs.  $\theta$  to the value  $\theta = 0$ . The values of interaction constants change from  $-3.24$  to  $-0.31$  for  $-6 < \sigma_M < +5$   $\mu\text{C cm}^{-2}$  in 0.1 mol dm<sup>-3</sup> NaClO<sub>4</sub>; from  $-3.87$  to  $-0.54$  in 1 mol dm<sup>-3</sup> NaClO<sub>4</sub>; from  $-12.67$  to  $-1.99$  in the same range of charges in 5 mol dm<sup>-3</sup> NaClO<sub>4</sub>. A similar effect occurs in the systems containing thiourea<sup>26,27</sup> and thiourea derivatives.<sup>4,25</sup>

In all the systems studied, the increase of  $\sigma_M$  is accompanied by a decrease of a repulsive interaction between the adsorbed dipoles of ATU and an increase of the adsorption energy (Figure 7). This is probably related to the increase of ClO<sub>4</sub><sup>-</sup> anions adsorbing near the positive pole of the polar ATU molecule and thus screening the repulsive forces between the adsorbed ATU molecules, which leads to increased ATU adsorp-

tion, which is indicated by the increase of  $\Gamma'$  (Figure 5). The linear dependence  $\Delta G = f(\sigma_M)$  (Figure 6) indicates the preferential participation of stable ATU dipoles which influence the value of free adsorption energy.<sup>28</sup> It should be emphasized that along with the increase of the supporting electrolyte concentration, the values of  $\Delta G^\circ$  increase and the repulsive interaction between the adsorbed dipoles of ATU also increases. This could suggest that the measure of the adsorption magnitude is a result of these two parameters, as shown in the dependences in Figure 5.

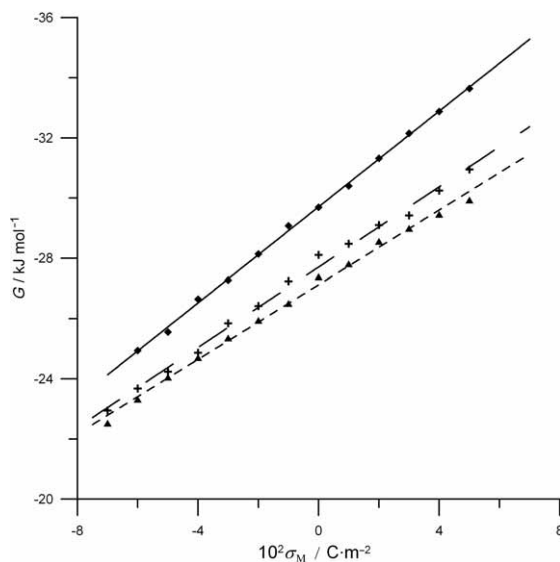


Figure 7. Energy adsorption of ATU as a function of the electrode charge for 0.1 mol dm<sup>-3</sup> NaClO<sub>4</sub> (▲), 1 mol dm<sup>-3</sup> NaClO<sub>4</sub> (+) and 5 mol dm<sup>-3</sup> NaClO<sub>4</sub> (■).

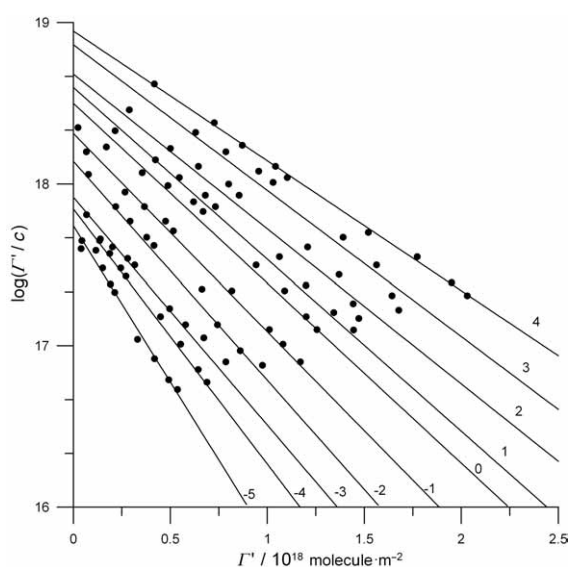


Figure 8. Linear test of the virial isotherm for the system 1 mol dm<sup>-3</sup> NaClO<sub>4</sub> + ATU. Electrode charges ( $\sigma_M$  in 10<sup>-2</sup> C m<sup>-2</sup>) are indicated by each line.

Virial isotherms were also used to describe the adsorption of ATU:

$$\ln \beta c = \Gamma' + 2B\Gamma' \quad (3)$$

where  $c$  is the molar concentration of ATU,  $B$  is the second virial coefficient.

The virial isotherm verifies the results obtained from the Frumkin isotherm, because calculation of the values of surface excess at saturation is not required in this case.

Figure 8 shows the linear test of the virial isotherm for the 1 mol dm<sup>-3</sup> NaClO<sub>4</sub> + ATU system. The values of the second virial coefficient  $B$  were calculated from the slopes of lines in Figure 8 and the corresponding  $\Delta G^\circ$  values were obtained from the intercepts of these lines with the axis  $\log(\Gamma'/c)$  using the standard state of 1 mol dm<sup>-3</sup> in bulk solution and one molecule on the surface. The obtained values of the virial isotherm constants are given in Table II.

TABLE II. Comparison of the virial isotherm constants for systems: 0.1 mol dm<sup>-3</sup> NaClO<sub>4</sub>, 1 mol dm<sup>-3</sup> NaClO<sub>4</sub> and 5 mol dm<sup>-3</sup> NaClO<sub>4</sub> containing ATU

$10^2 \sigma_M / \text{C m}^{-2}$	$-\Delta G^\circ / \text{kJ mol}^{-1}$			$B / \text{nm}^2 \text{ molecule}^{-1}$		
	0.1	1	5	0.1	1	5
-6	99.71	100.09	103.11	1.86	2.25	8.49
-4	101.78	101.80	103.79	1.34	1.58	2.97
0	103.20	103.48	105.35	1.04	1.35	2.14
+1	104.71	105.53	107.09	0.85	1.11	1.71
+3	105.55	106.08	107.89	0.80	1.06	1.65
+5	106.58	107.11	109.99	0.75	0.94	1.60
+5	107.21	108.08	110.53	0.69	0.80	1.46

Changes of  $\Delta G^\circ$  values as a function of the concentration of NaClO<sub>4</sub> and the electrode charge confirm analogous  $\Delta G^\circ$  changes obtained from the Frumkin isotherm. Increase of the  $\Delta G^\circ$  value with the increase of positive electrode charge could be related to the extraction of water molecules from the electrode surface. The obtained  $\Delta G^\circ$  values in 1 mol dm<sup>-3</sup> NaClO<sub>4</sub> at  $\sigma_M = 0$  are much higher than -95.7 kJ mol<sup>-1</sup> for thiourea adsorption from aqueous solution.<sup>26</sup> The values of the second virial coefficient  $B$  increase together with increasing supporting electrolyte concentration and the negative charge of the electrode.  $B$  values are higher than for the adsorption of thiourea,<sup>26</sup> *N,N'*-dimethylthiourea<sup>4</sup> and tetramethylthiourea,<sup>25</sup> especially in the range of negative charges of an electrode.

The modified Flory-Huggins isotherm<sup>29</sup> lasts more light on the adsorption mechanism determining the num-

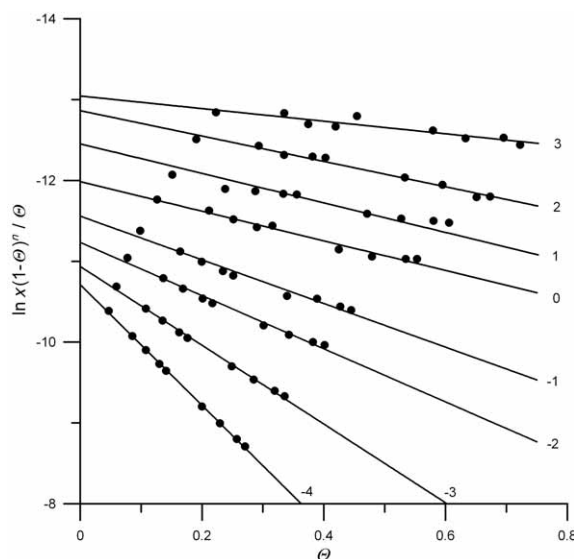


Figure 9. Test of the Flory-Huggins isotherm for the system 5 mol dm<sup>-3</sup> NaClO<sub>4</sub> + ATU. Electrode charges ( $\sigma_M$  in 10<sup>-2</sup> C m<sup>-2</sup>) are indicated by each line.

ber of water molecules displaced by one molecule of adsorbate:

$$\beta x = [\theta / n(1 - \theta)^n] \exp(-2A\theta) \quad (4)$$

where  $n$  is the number of water molecules replaced by one adsorbate molecule. In the presented case, involving use of a projected area of 0.123 nm<sup>2</sup> for water,<sup>30</sup>  $n$  was found to be 4.36–4.58 in all the systems studied.

Figure 9 presents the plots of  $\ln[x(1 - \theta)^n / \theta]$  versus  $\theta$  in the solution 5 mol dm<sup>-3</sup> NaClO<sub>4</sub> + ATU. The obtained values of  $\Delta G^\circ$  for all the systems studied were close to the corresponding values of  $\Delta G^\circ$  obtained from the Frumkin isotherm (Figure 6). However, the values of parameter  $A$  were higher compared to those obtained from the Frumkin isotherm. These differences can result from the divergence between the system studied and the model for the Flory-Huggins isotherm, in which the adsorbed species form a monolayer at the electrode interface with each molecule replacing  $n$  molecules of solvent. The values of parameter  $A$  decrease with the increase of the positive charge of the electrode, which is a result of penetration of ClO<sub>4</sub><sup>-</sup> anions among the positively charged amine groups of ATU at  $\sigma_M > 0$ <sup>6,7</sup> and, consequently, the screening of repulsive interactions between adsorbed ATU molecules, leading to an increase of ATU adsorption.

#### Electrostatic Parameters of the Inner Layer

Adsorption of ATU causes a change of the potential drop across the inner layer  $\Phi^{M-2}$ . Observation of these changes at a constant charge could be the source of information about the structure of a double layer. Accord-

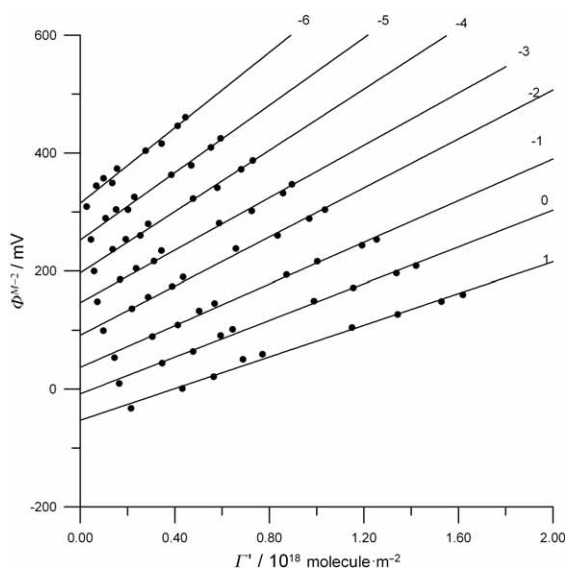


Figure 10. Potential drop across the inner layer  $\Phi^{M-2}$  as a function of the quantity of ATU adsorbed at constant electrode charges ( $\sigma_M$  in  $10^{-2}$  C  $m^{-2}$ ) for 0.1 mol  $dm^{-3}$  ATU.

ing to Parsons' electrostatic model,<sup>28</sup> the potential  $\Phi^{M-2}$  is the sum of two parts depending on the charge density and surface excess:

$$\Phi^{M-2} = \frac{4\pi x_1}{\epsilon_i} \sigma_M + \frac{4\pi \mu_{org}}{\epsilon_i} \Gamma'_{org} \quad (5)$$

where  $\mu_{org}$  is the dipole moment of an isolated adsorbed molecule ( $\mu_{ATU} = 17.04 \times 10^{-30}$  C m),<sup>8</sup>  $\epsilon_i$  is the dielectric constant of the inner layer and  $x_1$  is the inner layer thickness.

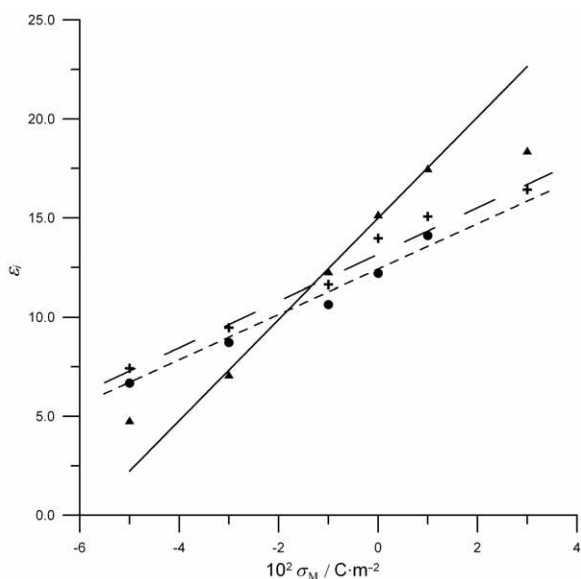


Figure 11. Apparent dielectric constant of the inner layer as a function of charges on the electrode for the systems: 5 mol  $dm^{-3}$   $NaClO_4$  (solid line), 1 mol  $dm^{-3}$   $NaClO_4$  (dashed line) and 0.1 mol  $dm^{-3}$   $NaClO_4$  (dotted line).

Dependence of  $\Phi^{M-2}$  on the surface excess  $\Gamma'$  at constant charge density for 0.1 mol  $dm^{-3}$   $NaClO_4$  is shown in Figure 10. Dependences  $\Phi^{M-2} = f(\Gamma'_{ATU})$  are linear in all the systems examined, which confirms the congruence of the described adsorption isotherms with the charge. It is important to note that the slope of lines in Figure 10 decreases when the charge increases. The ATU molecule negative end is oriented towards mercury even at the most negative values of  $\sigma_M$ , in spite of a very strong adsorption on mercury caused by the highly specific interaction between sulphur and mercury.

Linear dependences  $\Phi^{M-2} = f(\Gamma'_{ATU})$  were analyzed in a way similar to that used previously by Jurkiewicz-Herbich and Jastrzębska.<sup>31</sup> Values of the apparent dielectric constant of the inner layer  $\epsilon_i$  are presented in Figure 11. The  $\epsilon_i$  values increase with the positive charge of the electrode. The magnitude of  $\epsilon_i$  is comparable with the one obtained in solutions of 0.1 mol  $dm^{-3}$   $KNO_3$ <sup>26</sup> and 1 mol  $dm^{-3}$   $NaClO_4$ <sup>3</sup> containing thiourea. In the range of negative charges of the electrode, the lowest values of  $\epsilon_i$  were obtained in 5 mol  $dm^{-3}$   $NaClO_4$ . In the range of positive charges of the electrode, the values of  $\epsilon_i$  increased together with the increase of the supporting electrolyte

TABLE III. Inner layer properties for ATU adsorbed at mercury/aqueous solution  $NaClO_4$  interfaces for different supporting electrolyte concentrations.  $10^2 \sigma_M / C m^{-2}$ ;  $x_1 / nm$ ;  $K^i / 10^2 F m^{-2}$ ;  $\Gamma'_{ATU} / 10^{18} molecule m^{-2}$

$\sigma_M$	$\Gamma' = 0$		$\Gamma' = 1$		$\Gamma' = 1.5$	
	$K^i$	$x_1$	$K^i$	$x_1$	$K^i$	$x_1$
0.1 mol $dm^{-3}$ $NaClO_4$						
-5	17.86	0.33	12.02	0.49	-	-
-3	19.40	0.39	13.76	0.56	10.16	0.76
-1	20.32	0.46	15.23	0.62	12.02	0.78
0	21.37	0.50	16.41	0.65	13.34	0.81
+1	23.53	0.53	19.38	0.64	17.06	0.73
1 mol $dm^{-3}$ $NaClO_4$						
-5	13.99	0.44	9.94	0.62	-	-
-3	17.82	0.40	11.80	0.61	8.90	0.81
-1	20.41	0.46	13.25	0.70	11.63	0.79
0	20.52	0.64	14.81	0.89	12.59	1.05
+1	23.04	0.58	16.43	0.81	16.07	0.83
+3	32.82	0.39	21.89	0.61	21.74	0.62
5 mol $dm^{-3}$ $NaClO_4$						
-5	15.87	0.27	8.59	0.51	-	-
-3	17.42	0.36	10.27	0.62	8.34	0.75
-1	20.10	0.54	11.74	0.92	9.75	1.11
0	20.20	0.66	13.70	0.97	12.25	1.10
+1	22.35	0.69	15.13	1.02	14.04	1.11
+3	30.46	0.53	19.16	0.85	18.85	0.86

concentration, which indicates greater freedom of rotation of ATU molecules in the field of the double electric layer in case of lower water activity.

Calculated values of the integral capacity  $K^i$  and values of the inner layer thickness  $x_1$  are presented in Table III. Analysis of the results presented in Table III shows that the values of  $K^i$  increase with an increase of the electrode charge and decrease with an increase of the supporting electrolyte concentration and with an increase of surface concentration of ATU at all values of  $\sigma_M$  within the range studied. Decrease of the  $K^i$  value with the increase of ATU concentration is connected with the increase of the inner layer thickness. The determined inner layer parameters are slightly lower than those determined for thiourea from aqueous  $\text{NaF}^{28}$  and  $\text{NaClO}_4^{32}$  solutions.

Changes of adsorption parameters with the change of the supporting electrolyte concentration point to the competitiveness of ATU and  $\text{ClO}_4^-$  ions adsorption as well as to electrostatic interactions between ATU molecules and water.

## CONCLUSIONS

ATU adsorbs at the interface mercury/water solution of  $\text{NaClO}_4$ . The linear dependence  $E_z = f(\lg c_{\text{ATU}})$  (Figure 3) indicates the specific adsorption of ATU on mercury. The surface excess of ATU increases with the increase of ATU concentration and the increase of electrode charge. The negative end of ATU molecules is pointed towards the mercury, which is the result of the specific interaction between mercury and the sulphur of ATU. Such situation does not change even at negative values of electrode charge, which is shown by the decrease of the slope of linear dependence  $\Phi^{M-2} = f(\Gamma'_{\text{ATU}})$  (Figure 10) with an increase of the charge. Repulsive interactions exist among the ATU molecules adsorbed on mercury, which become weaker with increased electrode charge. The energy of adsorption increases together with the increase of electrode charge, which could be related to the removal of water molecules from the electrode surface at  $\sigma_M > 0$ .<sup>32</sup>

The shift of  $E_z$  values towards negative potentials in the solutions without ATU indicates that  $\text{ClO}_4^-$  ions are also adsorbed on mercury. Nevertheless, such adsorption is not specific, which is proved by the parallel course of lines  $E_z = f(\lg c_{\text{ATU}})$  in Figure 3. Participation of  $\text{ClO}_4^-$  ions in adsorption processes is also confirmed by the increase of  $\Delta G$  and  $B$  values with increasing supporting electrolyte concentration. However, the slight changes of the electrostatic parameters of the double layer, as the  $\text{NaClO}_4$  concentration increases, point to weak adsorption of  $\text{ClO}_4^-$  ions on mercury.

In addition, the results of the experiments indicate that the surface occupied by one molecule of ATU de-

creases together with an increase of  $\text{NaClO}_4$  concentration and the number of water molecules removed from the surface with one molecule of adsorbate increases. Although these changes are slight, they point to the presence of electrostatic interactions in the double layer between the dipoles of  $\text{H}_2\text{O}$  and ATU.

## REFERENCES

1. C. Buess-Herman, L. Gierst, and M. Gonze, *J. Electroanal. Chem.* **226** (1987) 267–281.
2. G. Dalmata, *Polish J. Chem.* **67** (1993) 2193–2203.
3. A. Nosal-Wiercińska, Z. Fekner, and G. Dalmata, *J. Electroanal. Chem.* **548** (2005) 192–200.
4. A. Nosal-Wiercińska and G. Dalmata, *Electrochim. Acta* **51** (2006) 6179–6185.
5. A. M. Morozow, N. B. Grigoriev, and I. A. Bagotskaja, *Elektrokhimya* **3** (1967) 585–590.
6. B. B. Damaskin, A. A. Surwiła, and Ł. E. Rybalka, *Elektrokhimya* **3** (1967) 927–934.
7. S. Ł. Diatkina and B. B. Damaskin, *Elektrokhimya* **8** (1972) 1123–1128.
8. I. Lukovits, I. Bako, A. Shaban, and E. Kalman, *Electrochim. Acta*, **43** (1998) 131–136.
9. R. A. Robinson and R. H. Stokes, *Electrolyte Solutions*, Butterworths, London, 1965.
10. R. M. Rush and J. S. Johnson, *J. Phys. Chem.* **72** (1968) 767–774.
11. Z. Galus, *Elektroanalityczne Metody Wyznaczania Stałych Fizykochemicznych*, PWN, Warszawa, 1979, pp.70–76.
12. D. C. Grahame, R. P. Larsen, and M. A. Poth, *J. Am. Chem. Soc.* **71** (1949) 2978–2983.
13. D. C. Grahame, E. M. Coffin, J. I. Commings, and M. A. Poth, *J. Am. Chem. Soc.* **74** (1952) 1207–1211.
14. D. J. Schiffrin, *J. Electroanal. Chem.* **23** (1969) 168–171.
15. A. De Battisti and S. Trasatti, *J. Electroanal. Chem.* **54** (1974) 1–17.
16. D. M. Mohilner and H. Nakadomari, *J. Phys. Chem.* **74** (1973) 1594–1595.
17. D. M. Mohilner, L. W. Browman, S. J. Freeland, and H. Nakadomari, *J. Electrochem. Soc.* **120** (1973) 1658–1662.
18. R. Parsons and R. Payne, *Z. Phys. Chem. (N. F.)* **98** (1975) 9–22.
19. R. Parsons, *Can. J. Chem.* **59** (1981) 1898–1902.
20. D. Schuhmann, R. Bennes, P. Vanel, and D. Bellostas, *J. Electroanal. Chem.* **101** (1979) 73–89.
21. R. Andreu, M. Sluyters-Rehbach, A. G. Remijnse, and J. H. Sluyters, *J. Electroanal. Chem.* **134** (1982) 101–115.
22. R. Parsons, *Trans. Faraday Soc.* **51** (1955) 1518–1529.
23. F. W. Schapink, M. Oudeman, K. W. Leu, and J. N. Helle, *Trans. Faraday Soc.* **56** (1960) 415–423.
24. O. Ikeda, H. Iimbo, and H. Tamura, *J. Electroanal. Chem.* **137** (1982) 127–141.
25. D. Gugala, Z. Fekner, D. Sienko, J. Nieszporek, and J. Saba, *Electrochim. Acta* **49** (2004) 2227–2236.
26. R. Parsons and P. C. Symons, *Trans. Faraday Soc.* **64** (1968) 1077–1092.
27. G. Pezzatini, M. R. Moncelli, and R. Guidelli, *J. Electroanal. Chem.* **301** (1991) 227–240.

28. R. Parsons, *Proc. Roy. Soc.* **79A** (1961) 261–269.  
29. S. Trasatti, *J. Electroanal. Chem.* **28** (1970) 257–277.  
30. J. Lawrence and R. Parsons, *J. Phys. Chem.* **73** (1969) 3577–3581.  
31. M. Jurkiewicz-Herbich and J. Jastrzębska, *Polish J. Chem.* **58** (1984) 1125–1137.  
32. R. Payne, *J. Electroanal. Chem.* **41** (1973) 145–157.

---

## SAŽETAK

### Adsorpcija *N*-aliltiouree na površinu živine elektrode: ovisnost o koncentraciji osnovnog elektrolita

Grażyna Dalmata i Agnieszka Nosal-Wiercińska

Istražen je utjecaj gustoće naboja na elektrodi i koncentracija adsorbata i osnovnog elektrolita na adsorpciju *N*-aliltiouree na granici faza živa/vodena otopina NaClO<sub>4</sub>. Mjereni su diferencijalni kapacitet dvosloja, potencijal nultog naboja i napetost površine žive pri tom potencijalu. Određeni su sljedeći adsorpcijski parametri: površinska koncentracija, slobodna energija adsorpcije, konstante interakcije i elektrostatski parametri unutrašnjeg sloja. Uočeno je da se adsorpcijski parametri mijenjaju s promjenom koncentracije osnovnog elektrolita, što ukazuje na kompetitivnu adsorpciju *N*-aliltiouree i ClO<sub>4</sub><sup>-</sup> iona i na elektrostatske interakcije među molekulama vode na površini elektrode.